



RESEARCH ARTICLE

Deep water recycling through time

10.1002/2014GC005525

Valentina Magni¹, Pierre Bouilhol¹, and Jeroen van Hunen¹¹Department of Earth Sciences, Durham University, Science Labs, Durham, UK

Key Points:

- Deep water recycling might be possible even in early Earth conditions
- We provide a scaling law to estimate the amount of H₂O flux deep into the mantle
- Subduction velocity has a major control on the crustal dehydration pattern

Supporting Information:

- Supporting Information Figures s01-s04
- Readme

Correspondence to:

V. Magni,
valentina.magni@durham.ac.uk

Citation:

Magni, V., P. Bouilhol, and J. van Hunen (2014), Deep water recycling through time, *Geochem. Geophys. Geosyst.*, *15*, 4203–4216, doi:10.1002/2014GC005525.

Received 24 JUL 2014

Accepted 8 OCT 2014

Accepted article online 14 OCT 2014

Published online 10 NOV 2014

This is an open access article under the terms of the Creative Commons Attribution-NonCommercial-NoDerivs License, which permits use and distribution in any medium, provided the original work is properly cited, the use is non-commercial and no modifications or adaptations are made.

Abstract We investigate the dehydration processes in subduction zones and their implications for the water cycle throughout Earth's history. We use a numerical tool that combines thermo-mechanical models with a thermodynamic database to examine slab dehydration for present-day and early Earth settings and its consequences for the deep water recycling. We investigate the reactions responsible for releasing water from the crust and the hydrated lithospheric mantle and how they change with subduction velocity (v_s), slab age (a) and mantle temperature (T_m). Our results show that faster slabs dehydrate over a wide area: they start dehydrating shallower and they carry water deeper into the mantle. We parameterize the amount of water that can be carried deep into the mantle, W ($\times 10^5$ kg/m²), as a function of v_s (cm/yr), a (Myrs), and T_m (°C): $W = 1.06v_s + 0.14a - 0.023T_m + 17$. We generally observe that a 1) 100°C increase in the mantle temperature, or 2) ~15 Myr decrease of plate age, or 3) decrease in subduction velocity of ~2 cm/yr all have the same effect on the amount of water retained in the slab at depth, corresponding to a decrease of $\sim 2.2 \times 10^5$ kg/m² of H₂O. We estimate that for present-day conditions ~26% of the global influx water, or 7×10^8 Tg/Myr of H₂O, is recycled into the mantle. Using a realistic distribution of subduction parameters, we illustrate that deep water recycling might still be possible in early Earth conditions, although its efficiency would generally decrease. Indeed, $0.5\text{--}3.7 \times 10^8$ Tg/Myr of H₂O could still be recycled in the mantle at 2.8 Ga.

1. Introduction

The fate of water in subduction zones is a key feature that influences the magmatism of the arcs and the recycling of volatiles. The water cycle through degassing and deep recycling via subduction zones is of primary importance for our understanding of the long-term exchange of water between the earth's interior and the exosphere. Fluids released from the slab at depth are most likely responsible for triggering mantle wedge melting and are therefore involved in the arc volcanism [Ringwood, 1974]. This is evidenced by the peculiar geochemistry of arc lavas [Tatsumi *et al.*, 2008] and by tomographic images that show low seismic velocities in the mantle wedge, which is interpreted as the partially molten or hydrated mantle wedge [Zhao *et al.*, 2009]. Moreover, the transport of water bound in hydrous minerals at great depths have a major impact on the Earth's volatile budget, on the chemical evolution of the Earth, and on the deep mantle composition and rheology [Shirey *et al.*, 2008].

The different metamorphic reactions that release fluids from the subducting plate can be studied with combined petrological and thermal models [Schmidt and Poli, 1998; Syracuse *et al.*, 2010; van Keken *et al.*, 2011; Wada *et al.*, 2012]. The depth at which the slab dehydrates depends on many factors that influence the thermal structure of the subduction zone, such as slab age, slab dip, subduction velocity, but also on the lithology of the slab and initial water content. Estimates of the amount of water that is released in the first 150 km from the slab have been suggested to range between about 40–70% [Rüpke *et al.*, 2004; Hacker, 2008; van Keken *et al.*, 2011; Parai and Mukhopadhyay, 2012]. This leaves a 30–60% of H₂O that can be carried deep into the mantle and recycled on long geological time scale. The large uncertainty on the amount of recycled water is mainly due to the poor constraints we have on some of the important factors listed above. In addition, the dehydration processes in subduction zones in the Archean or Hadean, have even larger uncertainties. This is mostly because our knowledge of the style of early Earth plate tectonics is limited. For instance, how fast plates were moving in the past is still debated. Some authors suggested that plates were faster and subduction was probably more episodic than today [van Hunen and van den Berg, 2008], others proposed that they were slower [Korenaga, 2013] or that there was no subduction at all in the Archean but instead a stagnant lid [Stern, 2008]. Another aspect that influences the efficiency of slab dehydration is the temperature of the mantle. Although different theories on the cooling of Earth suggest

different values of possible mantle temperature, it is commonly assumed that the Archean mantle was hotter by 100–300°C [Herzberg *et al.*, 2010]. Given the strong control of temperature on slab dehydration, it might have been difficult to carry water deep into the mantle in the early Earth.

Here we test this hypothesis through an extensive parameter sensitivity study, in which we vary slab age, velocity and mantle temperature in numerical models of subduction integrated with a thermodynamic database. First we calibrate results for present-day conditions by looking at how these parameters affect the dehydration processes in the crust and the lithospheric mantle of the subducting plate. Then, we investigate how these processes vary with mantle temperature. From this, we derive a parameterization of the amount of water that remains in the slab at large depths as a function of slab age, subduction velocity and mantle potential temperature. We find that the main factor that influences the onset and the area of slab dehydration is the subduction velocity: dehydration of fast slabs starts shallower, but ends deeper than for slow slabs. Moreover, we demonstrate that a significant amount of water can be carried by the slab deep into the mantle also in a hotter mantle, thus deep water recycling could have been operating in early Earth conditions.

2. Methodology

We investigate the dehydration pattern of a subducting slab through thermo-mechanical numerical models integrated with a thermodynamic database. We use the finite element code Citcom [Moresi and Gurnis, 1996; Zhong *et al.*, 2000; van Hunen *et al.*, 2005] to compute the thermal structure of the subduction system (Figure 1 and details in supporting information text). The metamorphic reactions in the slab and in the mantle wedge are modeled via a Gibbs free energy minimization strategy (Perple_X) [Connolly, 2005, 2009] that mainly uses the thermodynamic database of Holland and Powell [1998] (see Supporting Information text and P. Bouilhol *et al.*, A numerical approach to melting in warm subduction zones, submitted to *Earth Planetary Science Letters*, 2014 for details). For each composition (crust, lithospheric mantle and primitive mantle) we precalculate the equilibrium paragenesis for realistic ranges of P, T and H₂O content and store the results in look-up tables. Water is introduced at the inflow boundary and it is carried deeper by the ongoing subduction by passive tracers that are advected with the velocity field. These tracers hold the composition of the modeled lithologies and allow tracking the equilibrium mineral assemblages and changes in water content along the slab and in the mantle wedge. If dehydration reactions occur the water content of the tracer is updated, and therefore also its composition and stable assemblage. The free H₂O released by one or more tracers within one finite element, it is transferred upward and taken into account when calculating

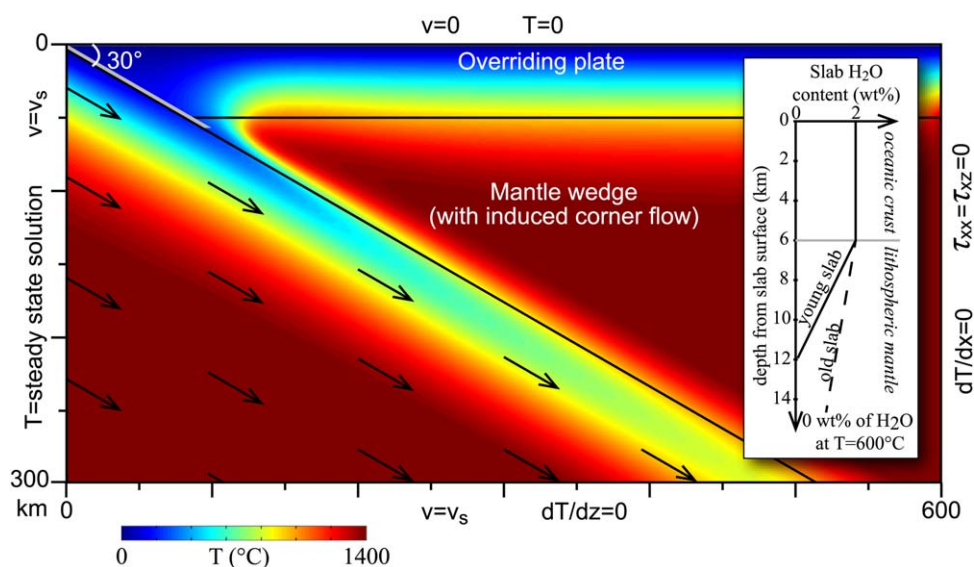


Figure 1. Schematic model setup geometry and boundary conditions. A rigid slab subducts at a constant dip of 30° and with a constant velocity prescribed at the left-hand side and bottom boundary. The slab is composed by a 6 km thick crust with 2 wt% of H₂O and a lithospheric mantle layer that is hydrated from 2 wt% at the Moho to 0 wt% at the 600°C isotherm. Colours indicate an example of the temperature field.

the phase assemblages in the element above. Rehydration can therefore occur in case there is any hydrous mineral in equilibrium at those specific P, T, and X conditions. Our models migrate water vertically upward, and do not consider the effect of the pressure gradient on fluids migration. Since we focus primarily on the slab dehydration and do not study the fate of fluid in the mantle wedge, except for the layer just above the slab surface, this is a good first order approximation [Gerya *et al.*, 2002; Arcay *et al.*, 2005; Wada *et al.*, 2008; Wada *et al.*, 2012].

The slab is formed by a 6 km layer of crust (LTBC sample in Schmidt and Poli, [1998]) that initially contains 2 wt% of water and a layer of depleted lithospheric mantle (DMM) [Workman and Hart, 2005]; the mantle wedge has a primitive mantle composition [Hart and Zindler, 1986]. To simulate a subducting serpentinized oceanic mantle lithosphere, part of the DMM is hydrated. The water content of the lithospheric mantle linearly decreases from 2 wt% at the Moho to 0 wt% at the 600°C isotherm [Rüpke *et al.*, 2004]. Therefore, the thickness of this hydrated layer changes with the thermal state of the subducting plate. At ~600°C serpentine is not stable anymore, thus water cannot be chemically bound in the lithospheric mantle, and brittle faulting may stop [Ranero and Sallarès, 2004]. Numerical models [Faccenda *et al.*, 2012] and seismic observations [Ranero *et al.*, 2003; Ranero and Sallarès, 2004] suggest that the normal faulting, due the bending of the slab at the trench, may extend until 20–40 km of depth, allowing a deep hydration of the slab. For instance in the Chile subduction zone the low seismic velocities of the Nazca plate are interpreted as a 20km thick lithospheric mantle layer with ~20% serpentinization at the top to ~15% at the bottom, which implies ~2.5 wt% of water [Ranero and Sallarès, 2004]. For both crustal and mantle lithologies, the calculated phase equilibria are in accordance and within errors of experimentally derived paragenesis (Figure s01). Nevertheless, our petrological model is limited by the available thermodynamic data and activity models for solid-solutions, and deviations from experiments might also arise from unconstrained oxygen fugacity and different starting composition. In the present case, for the lithospheric mantle one may expect serpentine to be stable at starting conditions. But for such low H₂O content (0–2 wt%), the predicted most stable assemblage is made of amphibole (Amph) and chlorite (Chl), serpentine being stable for H₂O > ~2.5 wt%; Figure s01). This has no effect on our global model since Chl breakdown is the last dehydration reaction to occur at high temperature (Figure s01). Similarly, at very high pressure, we cannot take into account the possible presence of phase 10Å [Fumagalli *et al.*, 2001; Fumagalli and Poli, 2005] or Mg-saussurite [Bromiley and Pawley, 2002; Komabayashi *et al.*, 2005] that would transport water from Chl-out to phase A. The P-T relationships among these phases are, however, experimentally uncertain. For our starting composition the calculations predict a transition from Chl-out to phase A through antigorite, thus alleviating the need of phase 10Å or Mg-saussurite to produce phase A.

3. Results

We perform a set of numerical models of subduction where slab age, subduction velocity and mantle potential temperature are varied to investigate how slab dehydration and deep water recycling could have been different in the early Earth compared to the present day. Subduction velocity is varied between 2.5 and 10 cm/yr, slab age between 40 and 80 Myr and the potential temperature between 1350 and 1550°C (see supporting information text and Figure s02 for a description of the effects of these parameters on the temperature field).

3.1. Dehydration Reactions

In our models we link the thermo-mechanical solution for a subduction system with the thermodynamic database that gives us the stable phase assemblages at different P, T and X conditions. We therefore have a tool that we can use to produce a paragenetic map of a subduction zone, allowing us to track the fate of water.

Such paragenetic map for a model with $v_s=5$ cm/yr, $a=40$ Myr and $T_m=1350^\circ\text{C}$ is shown in Figure 2a. The hydrated part of the lithospheric mantle is formed by a chlorite (Chl)-amphibole (Amph) bearing peridotite until a depth of about 95 km ($P < 30$ kbar). Deeper, amphibole is not stable, and bound water is only carried by chlorite until it breaks down. This occurs at depths >150 km (~48 kbar) at T around 600°C. This can also be observed in Figure 2c that shows how the amount of stable phases at the top and middle of the hydrated DMM layer changes with depth. The amount of Chl is initially ~15% at the top and ~8% in the middle. This difference is due to the fact that the water content linearly decreases from 2 wt% to 0 going

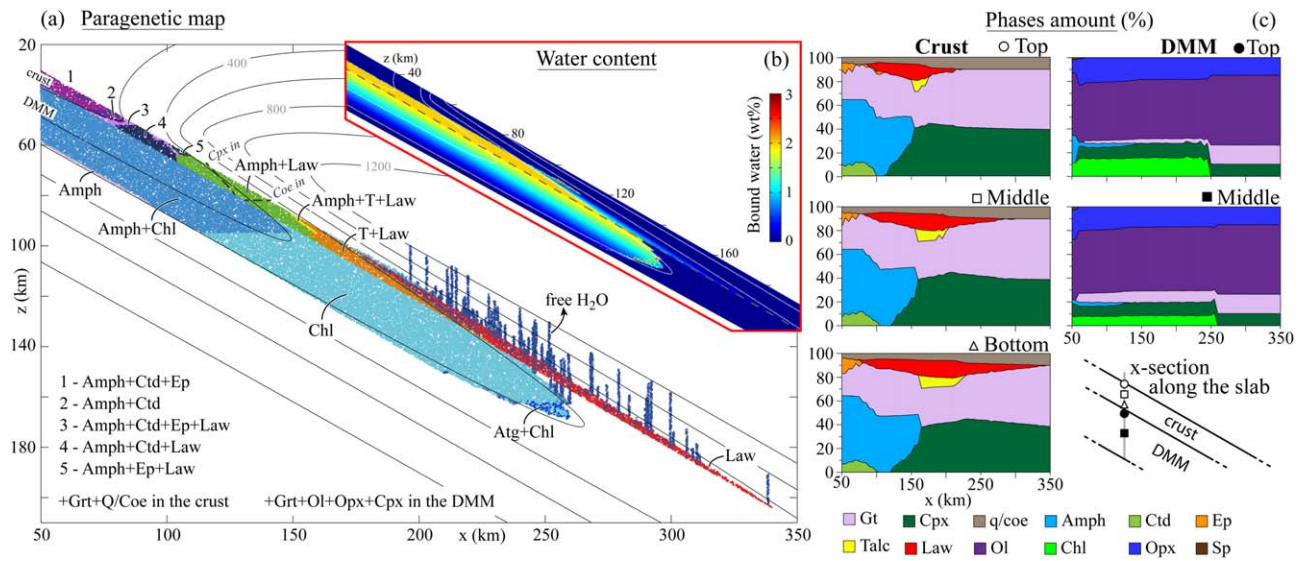


Figure 2. Results from model with $a=40$ Myr, $v_s=5$ cm/yr and $T_m=1350^\circ\text{C}$. (a) Paragenetic map: colours indicate different paragenesis along the slab; dry peridotite in the mantle wedge and in the slab mantle, and dry eclogite are left white; open blue circles show where free H_2O is present. Isotherms are showed every 200°C . (b) Bound water in the slab and mantle wedge; (c) phases amount (%) at the top, middle, and bottom of the crust (left column) and at the top and middle of the hydrated DMM layer (right column) along x sections, as shown in the schematic plot in bottom right corner.

deeper in the slab (Figure 2b, see Methodology section). Since the core of this hydrated DMM layer is colder than its edges, Chl remains stable for longer in the middle. Indeed, the dehydration of the lithospheric mantle, due to Chl breakdown, starts at ~ 150 km of depth at the edges until ~ 170 km in the middle (Figures 2a–2c). In a small area at the tip of the hydrated DMM, antigorite (Atg) becomes the hydrous stable phase in an Atg-Chl bearing peridotite (~ 160 km deep).

In the oceanic crust (Figures 2a–2c), the equilibrium phase assemblage from 50 to ~ 100 km depth is Amph-clinopyroxene (Cpx)-chloritoid (Ctd); until $z=66$ km)-garnet (Grt)-lawsonite (Law)-quartz (Q) or, deeper than ~ 84 km, coesite (Coe). Initially, until depths around 60 km, Epidote (Ep) is also stable in an amount of $\sim 10\%$. Water is therefore brought at depth by mainly Amph (50%), Ep, Ctd and Law, until Amph breaks down at ~ 100 km. At this point the hydrous minerals that are stable under these conditions are Law and talc. Although present in small amounts ($\sim 7\%$), talc breakdown, occurring along the 620°C isotherm from 95 km deep at the top of the slab to ~ 135 km at the bottom, is the first reaction that frees water from the crust. Deeper, lawsonite is the main hydrous phase that can hold water in the crust at higher P and T. Its breakdown occurs over a wide depth range as it starts at ~ 110 km (~ 36 kbar) and at temperatures higher than 650°C , occurring first at the top of slab, leaving a layer of dry Cpx-Grt-Coe eclogite residue that gets thicker with depth. The water content within the crust therefore gradually decreases as a function of lawsonite breakdown at increasing P, until the crust is completely dehydrated at a depth of ~ 200 km (Figure 2c). The water released from the talc and lawsonite breakdown reactions migrates upward and hydrates a thin layer of mantle wedge on top of the slab. This layer, which is at most 1 km thick, is made of an Amph-Chl bearing peridotite from ~ 95 to ~ 105 km and of a Chl bearing peridotite until ~ 120 km (Figure 2a).

3.2. Evolution of the Crust Dehydration Pattern

3.2.1. Present-Day Conditions: Effect of Subduction Velocity and Slab Age

The depths at which the crust first dehydrates (h_1) for models with different slab age and subduction velocity are shown in Figures 3a–3c. In the explored parameter space the range of first water release is 75–125 km. A clear inverse correlation is observed between h_1 and v_s (Figure 3a): for low v_s the crust starts to dehydrate deeper (108–125 km for $v_s=2.5$ cm/yr) than for high v_s (75–82 km for $v_s=10$ cm/yr). Although this might seem counterintuitive, it is a direct consequence of the fact that the top of the slab is hotter for faster subductions. This is because high subduction velocities create vigorous convection in the mantle wedge, causing the advection of heat to be very efficient. Thus, hot mantle material is brought very close to the top of the slab resulting in higher temperatures at shallower depths for fast slabs compared to the slower ones (see supporting information text and Figure s02). Slab age, on the other hand, has a weak

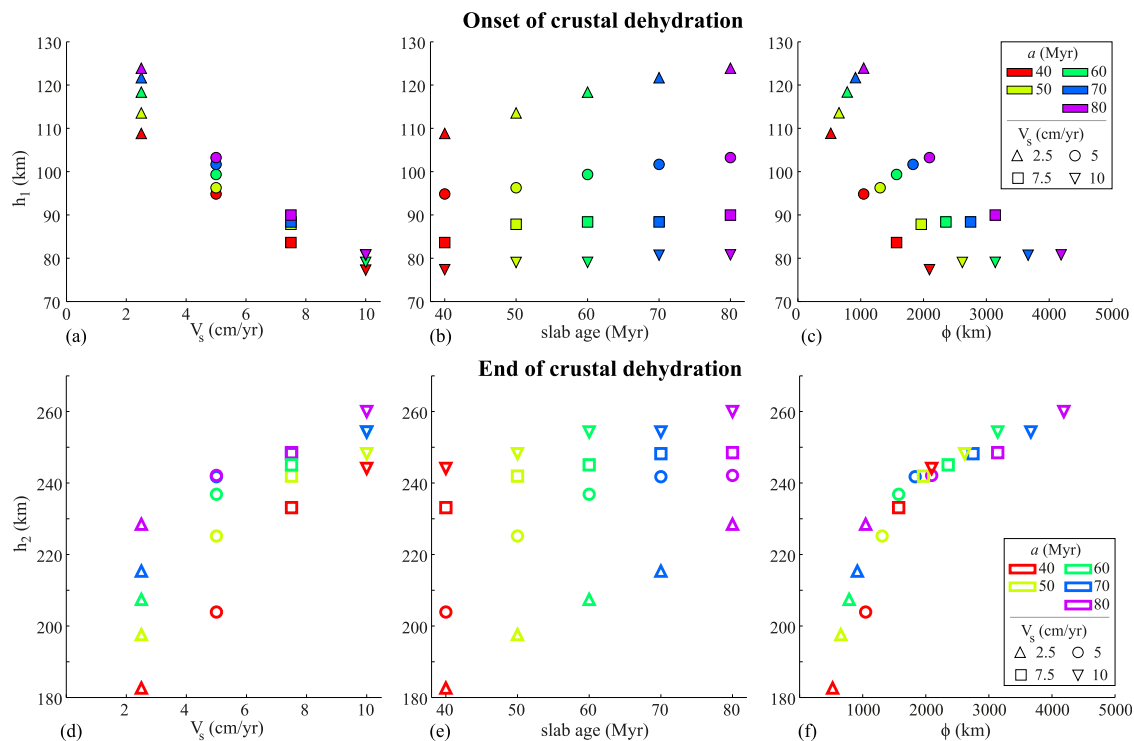


Figure 3. (a–c) Onset of crustal dehydration depths as a function of subduction velocity v_s , slab age a and thermal parameter ϕ , respectively. Colours indicate different slab ages, symbols show different velocities. A strong inverse correlation is found for the subduction velocity: the faster the slab subducts the shallower it starts to dehydrate. (d–f) End of crustal dehydration depths as a function of subduction velocity v_s , slab age a , and thermal parameter ϕ , respectively. Both v_s and slab age show a direct relationship with h_2 . The strongest correlation is found for the thermal parameter ϕ .

correlation with h_1 (Figure 3b). This is again related to the thermal structure of the subduction zone and the fact that the temperature at the top of the slab remains very similar when varying the plate age. Another parameter that is commonly used to describe the thermal state of a subduction zone is the thermal parameter ϕ [Kirby *et al.*, 1991], which is described as $\phi = av_s \sin(x)$. The dependency of the thermal parameter ϕ on h_1 is similar to the one observed for the subduction velocity, but the correlation here is less strong (Figure 3c). This is because ϕ is directly proportional to v_s (that has a strong correlation with h_1) and a (that has a very weak correlation with h_1).

The dehydration of the crust is a continuous process that lasts until lawsonite breakdown is totally achieved. This occurs between 180 and 260 km of depth in our models. As we did for the onset of the dehydration, we can examine the relationships between the different subduction parameters and the depth at which the crust is completely dry (h_2) (Figure 3d–3f). We find that both subduction velocity and slab age are directly proportional to h_2 , with v_s that shows a slightly stronger dependency than a . Fast and old slabs remain hydrated until deeper than slow and young ones. In this case, the strongest correlation is found with the thermal parameter ϕ : the higher the value of ϕ is, the deeper the crustal dehydration is completed (Figure 3c). The differences in these correlations compared to those found for the first water release, especially for the subduction velocity, result from the thermal structure of the system. Indeed, the crust dehydration starts from the top of the slab and, as the depth increases, it involves deeper parts of the crust. Therefore, subduction velocity plays a major role for h_1 , whereas for h_2 , also the slab age starts to have an effect. Moreover, crustal dehydration starts shallower for fast slabs and ends deeper, resulting in a much wider area, or a larger pressure range, where water is released from the slab into the mantle wedge.

3.2.2. Early Earth Conditions: Effect of a Hotter Mantle

So far we explored the effect of slab age and subduction velocity on the slab dehydration processes for models with a mantle potential temperature of 1350°C. However, the Archean mantle was likely to be hotter by ~ 200 K [Herzberg *et al.*, 2010]. Here we investigate how the crustal dehydration pattern changes for higher mantle potential temperature (1400°C, 1500°C, and 1550°).

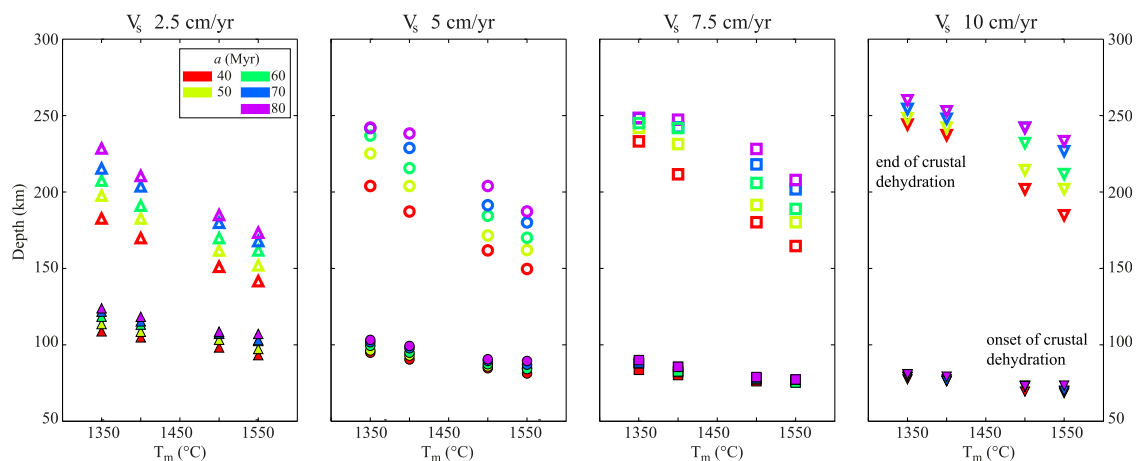


Figure 4. Onset (filled symbols) and end (open symbols) of crustal dehydration depths as a function of mantle potential temperature T_m . Colors indicate different slab ages, symbols show different velocities. An inverse relationship is found between T_m and both h_1 and h_2 .

For different slab ages and subduction velocities, the values of depths at which these reactions occur are different, as shown in Figure 4, where both the onset and the end of crustal dehydration are plotted for every model. There is an inverse relationship between T_m and both h_1 and h_2 : the higher the mantle potential temperature is, the shallower the crust starts and ends to dehydrate. For $T_m = 1550^\circ\text{C}$, the range of depths at which the crust starts to dehydrate is 70–107 km, and 142–233 km for the last water release depth. The correlations we found for the $T_m = 1350^\circ\text{C}$ cases with v_s and a are present also if T_m is varied.

3.2.3. Evolution of the Phases Involved in the Crust Dehydration

The P-T conditions under which the crust starts to dehydrate are not only important for the possible position of the volcanic arc, but are also crucial for the resulting composition of the fluids and the consequent characteristic signature that these fluids will give to the arc volcanism. Indeed, the P-T values and the resulting paragenesis when fluids are first released determine whether or not a particular mobile element would go into the fluid phase or will remain in the crust. Here we examine which are the phases involved in the first dehydration reactions for the different models.

Figure 5 shows the different modal proportions of minerals present at the top of the crust, as well as the first water free reaction, for all the models with plate age of 60 Myr. Although the increase of T_m and v_s has generally the same effect, increasing the velocity of the plate has a more drastic influence on the metamorphic crustal evolution. At the slab surface, the stability field of lawsonite decreases with the increase of subduction velocity and mantle potential temperature. Talc stability field is larger for slow subductions, where the temperature at the top of the slab is lower. With increasing T_m and v_s amphibole joins talc in the first water release reaction, and it then becomes the only phase that supplies free water with its breakdown. In all the models lawsonite is the next and last phase to breakdown. The main difference between present-day and early Earth conditions is found at $T_m = 1550^\circ\text{C}$ and $v_s = 10$ cm/yr (Figure 5), for which the breakdown of epidote releases the first water into the mantle wedge. This reaction occurs at $P \sim 22$ kbar with the following paragenesis: Cpx (22%), Gt (34%), Q (7%), Amph (30%), Ep (8%), and free H_2O .

Similar results are observed for different plate ages since this parameter has none or very little effect on the temperature at the top of the slab (see supporting information text and Figure s03). In some of the hottest models melting of the dry eclogitic crust occurs at the slab surface (at $z > 130$ km), triggered by the advection of metamorphic water coming from the breakdown of lawsonite and/or chlorite deeper in the slab (Bouilhol et al. submitted manuscript, 2014). The presence of this crustal melt does not affect the dehydration reaction evolution described above and, while potential important for the secular evolution of continental crust, it is beyond the scope of this work.

3.3. The Dehydration of the Lithospheric Mantle and the Deep Water Recycling

The way the slab lithospheric mantle dehydrates depends on the thermal structure of the subduction system and its initial water content. In the reference model (Section 3.2.1), hydrous phases in the slab mantle

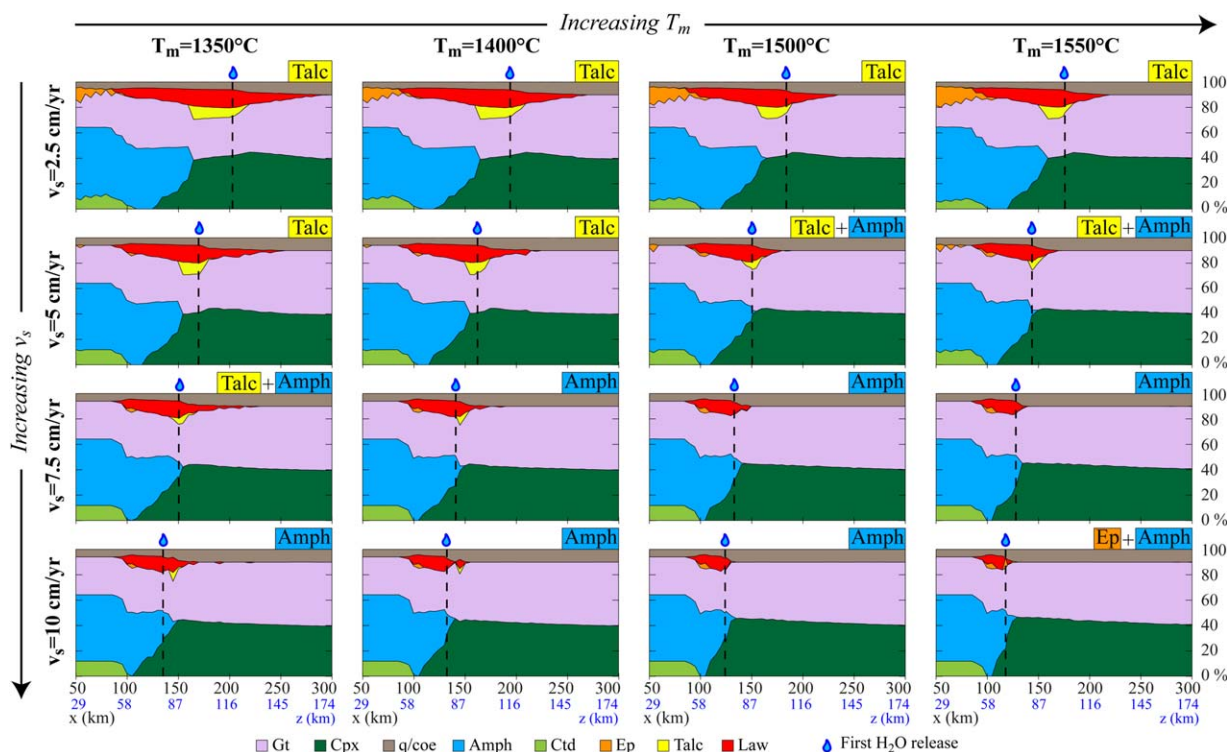


Figure 5. Evolution of the paragenesis in the crust at slab surface for all the models with $a=60$ Myr. Dashed lines indicate where the first dehydration reactions occur and the hydrous phase that frees H_2O is highlighted at the top right of each plot. In every model lawsonite is also involved in the dehydration.

are stable until temperatures around 600–650°C. If the slab is warm enough, all the water bound in the chlorite (or in the antigorite) will be released, leaving a completely dry peridotite. However, at high pressures ($P>60$ kbar or $z\sim 190$ km) and relatively low temperatures ($T<700^\circ\text{C}$), phase A is stable and can hold water [e.g., Thompson, 1992; Fumagalli and Poli, 2005; Komabayashi et al., 2005]. At even higher pressures the stability field of hydrous phases, such as phase A, phase E, hydrous phase B and ringwoodite, becomes wider and these phases are stable even at higher temperatures ($T\sim 1100^\circ\text{C}$) [Komabayashi and Omori, 2006]. Thus, if the DMM layer is still hydrated at pressures around 60 kbar, it is possible for the water to be carried deep into the mantle (see supporting information Figure s04). The deep water recycling, therefore, mainly depends on the appearance of phase A [Rüpke et al., 2004].

The different depths at which the lithospheric mantle completes its dehydration for every model are shown in Figure 6. When this value is 300 km (the maximum depth of our computational domain) it means that water is still present (in phase A) and it is expected to be carried deep into the mantle. Clearly the colder the slab is, the deeper the water can remain in the DMM. Therefore, for old and fast plates the conditions under which phase A is present are easy to reach. Indeed, when $v_s=10$ cm/yr and $T_m=1350^\circ\text{C}$, water is retained in the slab until deeper than 300 km in all the models except when the slab is fairly young (40 Myr). On the other hand, none of the models with very slow slabs ($v_s=2.5$ cm/yr) is able to hold water deeper than 155–180 km, depending on the age of the plate. This is because all the chemically bound water is released before phase A can be stable. The older the slab is, the larger the depth of the last water released is, and this is true for any subduction velocity or mantle potential temperature. In some cases (e.g., $a=70$ Myr and $v_s=5$ cm/yr) the lithospheric mantle is completely dry between 250 and 300 km of depth, meaning that although the phase A stability field is reached around 190 km, the dehydration continues, as the geotherm is parallel to the reaction boundary, and consumes all the bound water before the 300 km depth is reached. Interestingly, even for the highest mantle potential temperature of 1550°C, some models manage to reach the conditions to carry water at large depths. This occurs for $v_s=10$ cm/yr and $a=70$ –80 and for $v_s=7.5$ cm/yr and $a=80$.

We can now calculate how much of the initial water that enters the subduction zone remains within the slab at large depths and will therefore be transported deep into the mantle. For every model we compute

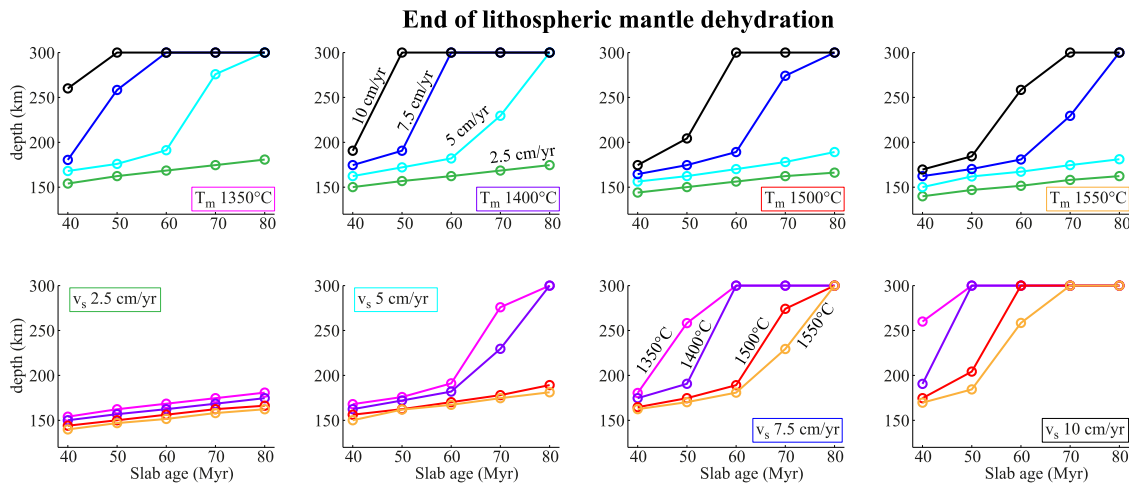


Figure 6. Depths of the end of dehydration of the lithospheric mantle layer for all the models. Colours indicate different subduction velocities in the first row and mantle potential temperature in the second row. When symbols are at 300 km (height of the computational domain) water is still present within the lithospheric mantle. Relatively young slabs ($a=40$ Myr) and very slow plates ($v_s=2.5$ cm/yr) always dehydrates before at $z<250$ km. At $T_m=1550^\circ\text{C}$ some models are not completely dehydrated at $z<300$ km.

the amount of water still bound in the slab in a column perpendicular to the slab surface where the depth of the slab surface is about 250 km, and we compare it to the one of a column at $z\sim 50$ km where slab dehydration has not started yet. Note that the initial water content of the slab varies for different models, as the

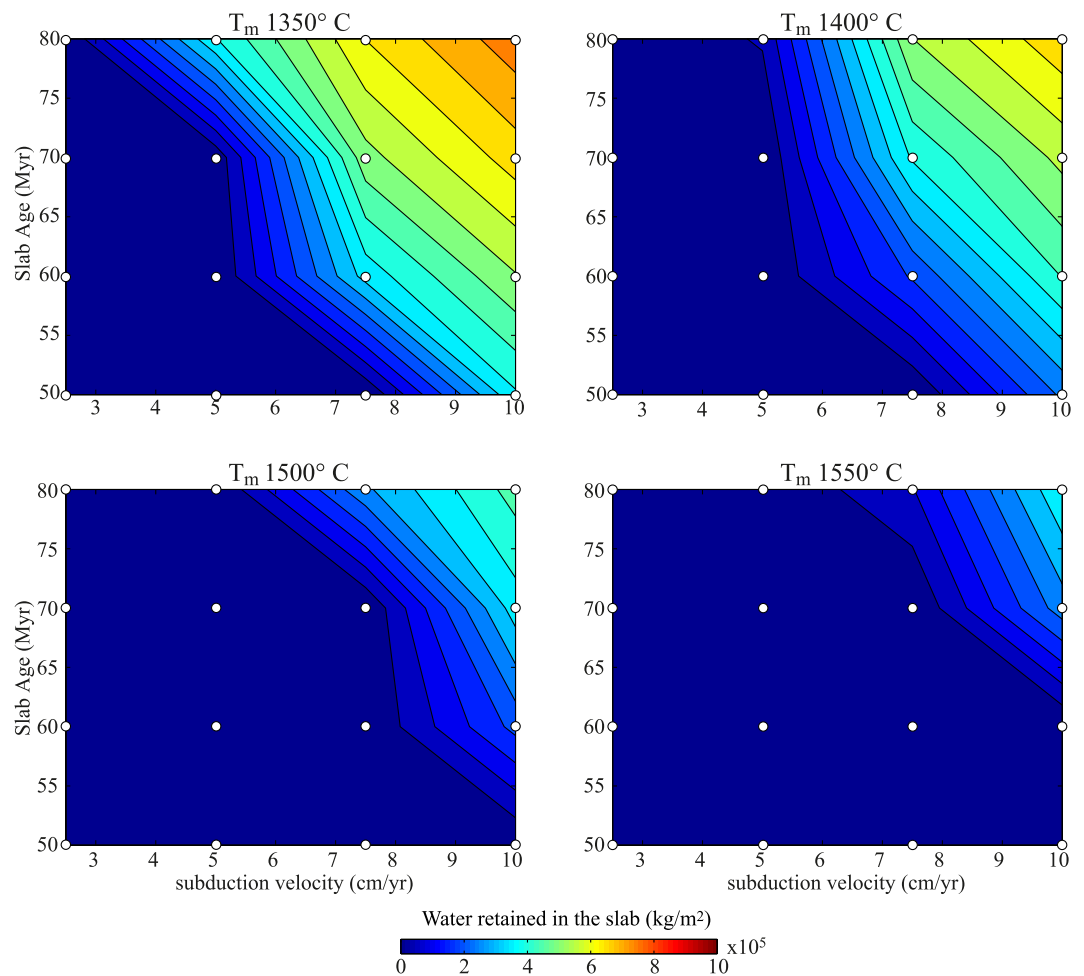


Figure 7. Contour plots of the amount of H_2O retained in the slab at depth ($z>250$ km) for all the models (white circles).

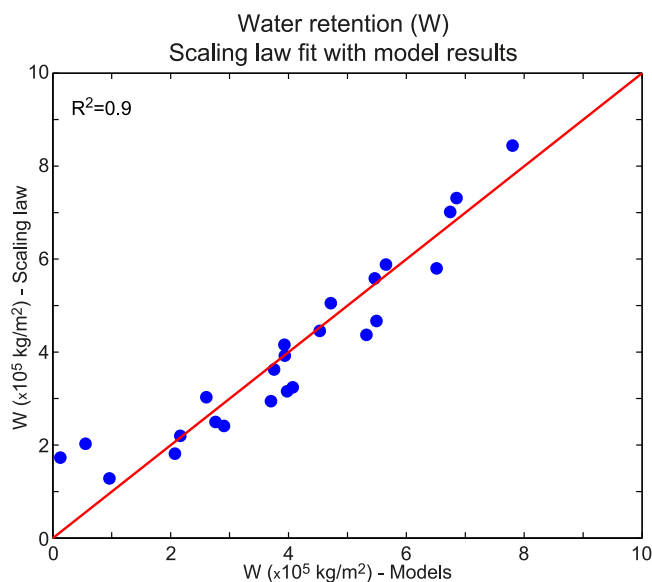


Figure 8. Amount of H₂O retained in the slab at $z > 250$ km obtained in the models (x axis) against those calculated with equation (1) (y axis).

The amount of water that stays in the slab (W) gradually decreases with decreasing slab age, subduction velocity and increasing mantle potential temperature for the models where phase A is present. We quantify the relationship between W ($\times 10^5$ kg/m²) and the explored parameters by fitting the results to the following scaling law:

$$W = 1.06v_s + 0.14a - 0.023T_m + 17 \quad (1)$$

with v_s is in cm/yr, a in Myr and T_m in °C. We observe that a 100°C increase in the mantle temperature and ~2 cm/yr decrease in the subduction velocity have the same effect on the amount of retained water, corresponding to a decrease of $\sim 2.2 \times 10^5$ kg/m². The same decrease is obtained when the slab is ~15 Myr younger. Figure 8 shows the fit between the model results and the values obtained by this scaling law, for which we obtain a R^2 value of 0.9.

4. The Water Cycle Evolution

We showed that the style of subduction strongly affects the amount of water retained in the slab at large depths. The style of plate tectonics and mantle convection may have changed in time, but in what way is still a matter of debate. *Korenaga* [2008] suggest that the average velocity of subducting plates decreased in time, which, together with the increasing mantle potential temperature, would make the deep water recycling difficult. On the other hand, *van Hunen and van den Berg* [2008] suggested that with an increase of mantle temperature of 100–200°C plates could move twice as fast as they do today, but that further mantle temperature increase would slow down subduction rates. Here we quantify the amount of water, W , carried deep into the mantle for these different proposed models of plate tectonic style by using the parametric law obtained from our results (Eq. 1).

We use the present-day distribution of subduction zones from *van Keken et al.* [2011] and, for the lack of precise information of this distribution for the early Earth, we assume this distribution to have remained constant through time. We fit the petrological estimates of mantle potential temperature of nonarc basalts (excluding komatiites) of *Herzberg et al.* [2010] to infer the thermal evolution of the mantle (Figure 9a). For each subduction zone we assume a water influx that depends on the thermal state of the slab, as we did in our numerical models. In this way we take into account the fact that less water can be stored in warm subduction zones.

We first calculate the amount of retained water in a case where only the mantle potential temperature changes with time, whereas plate velocities and ages remain constant compared to today subduction zone

thickness of the hydrated DMM layer depends on the position of the 600°C isotherm at the left hand side boundary (see Section 2). For instance, in the model with a young slab ($a = 40$ Myr and $T_m = 1350^\circ\text{C}$) the absolute value of water held in the slab is 9.8×10^5 kg/m², whereas for an 80 Myr old slab it is 1.3×10^6 kg/m². Our results show that in the coldest case scenario (i.e., $a = 80$ Myr, $v_s = 10$ cm/yr, and $T_m = 1350^\circ\text{C}$) 7.8×10^5 kg/m² of H₂O are recycled deep into the mantle (Figure 7). This means that in this case ~58% of the initial bound water remains in the slab. Even with a 200°C hotter mantle is still possible to recycle up to 3.9×10^5 kg/m² of H₂O, or ~34%.

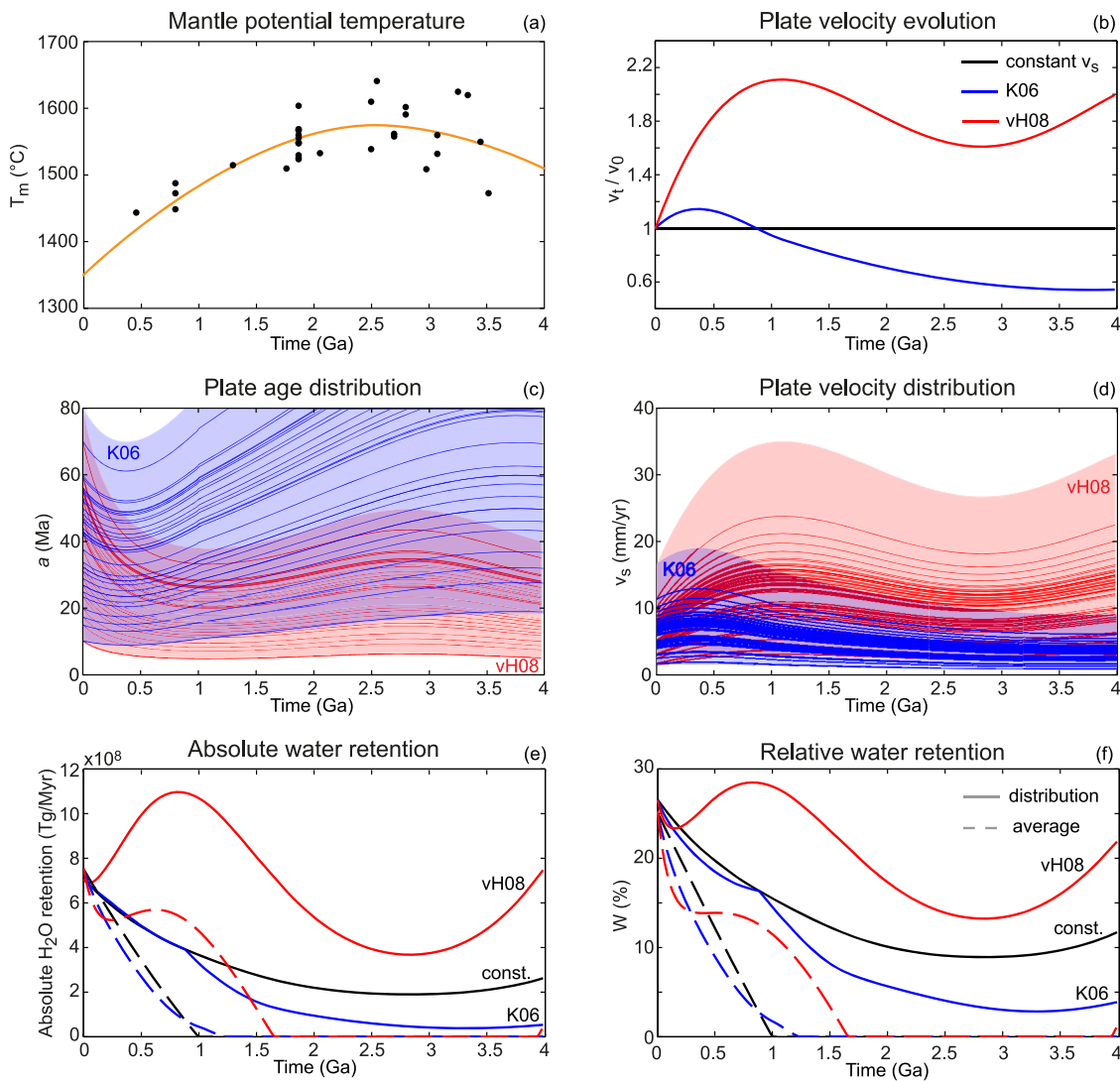


Figure 9. Water retention in deep time. (a) Potential mantle temperature evolution in time: the orange line is a fit of the data points of petrological estimates of potential mantle temperature of nonarc lavas from *Herzberg et al.* [2010]. (b) Plate velocity evolution in time for different models: in constant v_s , plate velocities remain the same as today from *van Keken et al.* [2011] compilation, K06 is the model suggested by *Korenaga* [2006], and vH08 is the model suggested by *van Hunen and van den Berg* [2008]. (c, d) plate age and velocity distribution as they would evolve from the present-day values following the models showed in Figure 9b. (e, f) Estimates of the evolution in time of the absolute and relative water retention for the different models, considering the distribution of subduction zones (solid lines) or an average value (dashed lines).

distribution. Note that at any time we are not using a single value of v_s and a , but instead compute the water retention for each subduction zone, thus taking into account the entire distribution. A maximum plate age of 80 Ma is assumed, since the plate model [*Parsons and Sclater, 1977*] would result in roughly constant ‘apparent age’ for older plates [*Ritzwoller et al., 2004; van Hunen et al., 2005*]. We estimate that for the present-day conditions a $\sim 26\%$ of the influx water, or 7×10^8 Tg/Myr, is carried by the slab at depths >250 km (Figures 9e–9f). With increasing T_m with time the water retention decreases, and W reaches an almost steady state value of 1.9×10^8 Tg/Myr at 2.5 Ga (Figure 9e). This model argues that if the style of plate tectonics has always been the same, deep water recycling has always been possible, although less efficient in the past, during the entire Earth evolution.

If plates were moving with different velocities compared to today, different estimates of water retention in the slab are obtained. For the two proposed models of plate velocity evolution we compute subduction velocity and plate age of each subduction zone as

$$v_s = v_{s0} * (v_t/v_{t0}) \quad (2)$$

$$a = a_0 / (v_t / v_{t_0}) \quad (3)$$

where $v_{s,0}$ and a_0 are the present-day plate velocities and ages of each subduction zone, and the ratio v_t/v_{t_0} describes how much plate velocity (v_t) changes at any time compared to the one estimated for the present day (v_{t_0}) (Figure 9b). With the plate velocity evolution suggested by *Korenaga* [2008], W decreases from 26 to 7% (1.4×10^8 Tg/Myr) at 1.5 Ga and reaches values $< 0.5 \times 10^8$ Tg/Myr from about 2.7 Ga. In the model proposed by *van Hunen and van den Berg* [2008], W increases until it reaches a maximum of 10.9×10^8 Tg/Myr (28%) around 0.8 Ga, corresponding to the peak in plate velocity, and then decreases to its minimum value for this model (3.7×10^8 Tg/Myr) at ~ 2.8 Ga, as an increase of T_m of $> 200^\circ\text{C}$ corresponds to a velocity decrease. However, at even older times (> 2.8 Ga) the mantle potential temperature decreases (according to the used model), resulting in a new increase in plate velocity and in the H_2O flux into the deep mantle (Figure 9).

To illustrate the importance of taking into account the variety of plate ages and velocities (which we know exists today and, most likely, existed in the past too), we repeated the same calculations described in the previous paragraph with one, average value of plate velocity ($v_{s,0} = 6.1$ cm/yr) and plate age ($a_0 = 71$ Ma), instead of considering the subduction zones distribution. Results are dramatically different, as for all the three models the amount of water retention would decrease rapidly and no water would be recycled deep into the mantle before 1–1.6 Ga (dashed lines, Figures 9e and 9f).

5. Discussion

Our results show that subduction velocity has a major control on the crustal dehydration, whereas the age of the plate has a very little effect. Indeed, the faster the plate is subducting the shallower it starts dehydrating, because of the vigorous mantle wedge convection generated by fast subduction that brings hot mantle material close to the slab surface. Therefore, although a slab is commonly considered to be cold if it is subducting fast, this is not the case when looking at the temperature at the slab surface. Furthermore, we find that for higher subduction velocity the depth range of crustal dehydration is wider. This would produce a larger area of partial melting in the mantle wedge and is likely to have an effect on the width of the arc. Indeed, this seems to fit well natural examples like the Japan and Kamchatka subduction zone, where the subduction velocity is quite high (8.3 cm/yr and 7.7 cm/yr, respectively) and volcanoes are present almost 100 km landward of the volcanic arc [*Wada and Wang*, 2009].

The strong relationship we find between subduction velocity and the depth of first water release and the very poor one with slab age is consistent to what found by *England et al.* [2004]. In their work, *England et al.* showed that the depth of the slab beneath arc volcanoes correlates neither with age of the descending ocean floor nor with the thermal parameter of the slab, whereas it exhibits an inverse correlation with subduction velocity. Although the depth of the slab beneath the arc and the beginning of the dehydration in the slab cannot be directly compared, it is commonly accepted that these features are related to each other since the fluids released from the slab are responsible for triggering mantle wedge melting and are, therefore, related to the arc volcanism.

In an early Earth setting, with a hotter mantle, we find that epidote is responsible for releasing water for fast subductions, as the crustal dehydration starts slightly shallower than in the present-day conditions. However, apart from this particular case, we do not find major differences in the metamorphic reactions occurring along the slab between the early Earth and the present-day conditions. With a hotter mantle, and keeping the other parameters fixed, the crustal dehydration starts shallower, and involves amphibole instead of talc, but similar results can be obtained by varying the subduction velocity. However, if in the early Earth subduction was generally faster, the role of epidote in crustal dehydration might have been more important than today. Such evolution may have a drastic impact on the fluid composition that is released.

In our study we consider the changes in the thermal structure of the slab created by three parameters (v_s , a , and T_m). However other factors can influence the temperature field and, thus, the slab dehydration processes, such as the slab dip, the thickness of the overriding plate, the rheology of the mantle wedge, and the composition of subducting plate. Although a more complex and realistic rheology would include, for instance, dislocation creep as a possible deformation mechanism and shear heating, we think their effect on our results is negligible. *Van Keken et al.* [2008] showed that very similar temperature fields are obtained

when considering only diffusion creep or both diffusion and dislocation creep as deformation mechanisms. Shear heating might have an effect on the slab temperature, but its influence is particularly significant where the plates are coupled and where temperatures in the subduction shear zone do not exceed the brittle-plastic transition [Peacock, 1994]. The effect of shear stresses on the temperature would be therefore more important at the shallow depths (<50–60 km).

5.1. Implications for the Global Water Cycle

In our calculations the slab is formed by two layers: a uniformly hydrated crust (2 wt% of H₂O) and a lithospheric mantle with a water content that linearly decrease with depth (2–0 wt% of H₂O). If we use the compilation of the subduction zones by *van Keken et al.* [2011] this results in a total flux of H₂O entering the trench of 2.6×10^9 Tg/Myr, with 0.86×10^9 Tg/Myr carried by the crust and 1.74×10^9 Tg/Myr by the lithospheric mantle below. Many uncertainties exist on the initial hydration state of an incoming plate and different authors used different settings in their calculation of the global H₂O influx. Although our estimates are quite high, they are included in the very wide range of values suggested in the literature: $0.7\text{--}2.1 \times 10^9$ Tg/Myr [*van Keken et al.*, 2011], $1.33\text{--}2.4 \times 10^9$ Tg/Myr [*Hacker*, 2008], $2.41\text{--}3.76 \times 10^9$ Tg/Myr [*Faccenda et al.*, 2012], $0.8\text{--}1.8 \times 10^9$ Tg/Myr [*Rüpke et al.*, 2004] (see *Faccenda* [2014] for a more detailed compilation).

We estimate that at the present-day conditions 26% of the water entering the trench can be retained in the slab, particularly in phase A in the lithospheric mantle, and carried deep into the mantle. This results in a return flux of H₂O in the mantle of 0.7×10^9 Tg/Myr (Figure 9e). Our estimates are consistent with previous suggested values, although toward the high end of the range: $0.33\text{--}0.43 \times 10^9$ Tg/Myr [*van Keken et al.*, 2011], 0.84×10^9 Tg/Myr [*Hacker*, 2008], $0.27\text{--}0.65 \times 10^9$ Tg/Myr [*Faccenda et al.*, 2012], $0.0\text{--}0.7 \times 10^9$ Tg/Myr [*Rüpke et al.*, 2004], $0.25\text{--}0.63 \times 10^9$ Tg/Myr [*Parai and Mukhopadhyay*, 2012]. Note that in each of these studies the depth at which the water is considered to be carried deep into the mantle is different. For instance, the estimates of *Hacker* [2008] are for $P > 4$ GPa (~ 120 km), whereas for *van Keken et al.* [2011] and *Rüpke et al.* [2004] are for depths larger than 230–240 km. In our estimates we calculate the amount of water still present in the slab at depths > 250 km. This is where, in our models, the crust is already completely dehydrated and the water is chemically bound in the DMM because of the presence of phase A, which will continue to be stable at larger depths as well.

We do not consider the possibility for the water to be bound in the nominally anhydrous minerals (NAMs). In an eclogitic crust NAMs can hold from few hundreds of ppm to 0.1–0.2 wt% [*Bolfan-Casanova*, 2005; *Smyth and Jacobsen*, 2006; *Faccenda*, 2014], whereas in the upper mantle the H₂O storage capacity of NAMs increases with depth from $\sim 0.1\text{--}0.2$ at 120 km to $0.4\text{--}0.55$ at the 410 km [*Hirschmann et al.*, 2005]. Our estimates of global H₂O flux might therefore underestimate the amount of H₂O that remains trapped in the mantle and it is not recycled. However many uncertainties exists in these experimental measurements. Moreover, the water content in the NAMs is likely to decrease for higher temperatures [*Hirschmann*, 2006], and it is therefore difficult to infer how these values might have been different in deep times.

Models with a 100–200°C hotter mantle show that, if the plate is old and fast enough, it is still possible to have some water retained in the slab. Results show that a $\sim 2.2 \times 10^5$ kg/m² decrease in the value of H₂O retained in the slab at depth can be obtained with an increase of 100°C of the mantle temperature, a decrease of ~ 2 cm/yr of the subduction velocity and a decrease of the slab age of ~ 15 Myr. Therefore, a hotter mantle is not enough to prevent deep water recycling, as an increase of few cm/yr of the subduction velocity can be enough to stabilize phase A even with a 1550°C mantle potential temperature. Our estimates of the evolution of water retention in time suggest that at 2.5 Ga 3–13% of initial H₂O could still be carried deep into the mantle. We predict that the global water flux deep into the mantle from 4 Ga until today is about one present-day ocean mass in the case of constant plate age and velocity (black lines in Figure 9), 60% of the ocean mass if the plate velocity was generally lower than today (blue lines in Figure 9), and two ocean masses if the plate velocity was generally higher than today (red lines in Figure 9). Interestingly, although the plate velocity evolution models we used are in contrast with each other, they both result in the possibility to have deep water recycling in the early Earth. This is the case when we take into account a range of different plate age and velocity values, which is more realistic than using only an average value. The importance of considering the distribution of subduction zones is well illustrated in the work of *Hacker* [2008] where he shows that nowadays few subduction zones (Andes, Tonga-Kermadec, Solomon, and Java-Sumatra-Andaman) are responsible for carrying almost 60% of the total return flux of H₂O in the mantle.

6. Conclusions

We present a numerical tool that can provide information on the P-T-X conditions of the slab dehydration process by combining thermo-mechanical models with a thermodynamic database. Moreover, we explore these conditions for a wide range of possible subduction systems, as we systematically vary the slab age, the subduction velocity and the mantle potential temperature. We draw the following conclusions.

1. Subduction velocity is the most important factor that affects the temperature at the slab surface and it has, thus, a major control on the crustal dehydration, especially its onset. Moreover, the faster the plate is subducting, the wider is the area affected by crustal dehydration.
2. The first crustal dehydration reaction is amphibole breakdown for fast plates, and, it involves talc as subduction speed decreases.
3. A hotter mantle (i.e., early Earth setting) drives the onset of crustal dehydration slightly shallower, but, mostly, dehydration reactions are very similar to those occurring in present-day setting. However, for very fast slabs and very hot mantle epidote is involved as a dehydrating crustal phase.
4. We provide a scaling law to estimate the amount of water that can be carried deep into the mantle. We find that an increase of 100°C in the mantle temperature or a decrease of ~15 Myr in the plate age have the same effect on the amount of water retained in the slab of a decrease of ~2 cm/yr in the subduction velocity.
5. Deep water recycling might be possible even in early Earth conditions, and, although its efficiency would generally decrease, we estimate that 3–13% of the initial water could still be recycle in the mantle at 2.5 Ga.

Acknowledgments

The authors would like to thank the reviewers Tetsuya Komabayashi and Manuele Faccenda, whose comments greatly improved the manuscript. We thank editor Yusuke Yokoyama and associate editor Paul Asimow for their constructive comments. This research was supported by the European Research Council (ERC StG 279828). This work made use of the facilities of N8 HPC provided and funded by the N8 consortium and EPSRC (grant EP/K000225/1). The Centre is coordinated by the Universities of Leeds and Manchester. We thank Lars Kaislaniemi for his contribution in developing the numerical tool.

References

- Arcay, D., E. Tric, and M. P. Doin (2005), Numerical simulations of subduction zones, *Phys. Earth Planet. Inter.*, 149(1–2), 133–153.
- Bolfan-Casanova, N. (2005), Water in the Earth's mantle, *Mineral. Mag.*, 69(3), 229–257.
- Bromiley, G., and A. Pawley (2002), The high-pressure stability of Mg-sursassite in a model hydrous peridotite: A possible mechanism for the deep subduction of significant volumes of H₂O, *Contrib. Mineral. Petrol.*, 142(6), 714–723.
- Connolly, J. A. D. (2005), Computation of phase equilibria by linear programming: A tool for geodynamic modeling and its application to subduction zone decarbonation, *Earth Planet. Sci. Lett.*, 236(1–2), 524–541.
- Connolly, J. A. D. (2009), The geodynamic equation of state: What and how, *Geochem. Geophys. Geosyst.*, 10, Q10014, doi:10.1029/2009GC002540.
- England, P., R. Engdahl, and W. Thatcher (2004), Systematic variation in the depths of slabs beneath arc volcanoes, *Geophys. J. Int.*, 156(2), 377–408.
- Faccenda, M. (2014), Water in the slab: A trilogy, *Tectonophysics*, 614, 1–30.
- Faccenda, M., T. V. Gerya, N. S. Mancktelow, and L. Moresi (2012), Fluid flow during slab unbending and dehydration: Implications for intermediate-depth seismicity, slab weakening and deep water recycling, *Geochem. Geophys. Geosyst.*, 13, Q01010, doi:10.1029/2011GC003860.
- Fumagalli, P., and S. Poli (2005), Experimentally determined phase relations in hydrous peridotites to 6–5 GPa and their consequences on the dynamics of subduction zones, *J. Petrol.*, 46(3), 555–578.
- Fumagalli, P., L. Stixrude, S. Poli, and D. Snyder (2001), The 10 Å phase: A high-pressure expandable sheet silicate stable during subduction of hydrated lithosphere, *Earth Planet. Sci. Lett.*, 186(2), 125–141.
- Gerya, T. V., B. Stöckhert, and A. L. Perchuk (2002), Exhumation of high-pressure metamorphic rocks in a subduction channel: A numerical simulation, *Tectonics*, 21(6), 1056, doi:10.1029/2002TC001406.
- Hacker, B. R. (2008), H₂O subduction beyond arcs, *Geochem. Geophys. Geosyst.*, 9, Q03001, doi:10.1029/2007GC001707.
- Hart, S. R., and A. Zindler (1986), In search of a bulk-Earth composition, *Chem. Geol.*, 57(3–4), 247–267.
- Herzberg, C., K. Condie, and J. Korenaga (2010), Thermal history of the Earth and its petrological expression, *Earth Planet. Sci. Lett.*, 292(1–2), 79–88.
- Hirschmann, M. M. (2006), Water, melting, and the deep Earth H₂O cycle, *Annu. Rev. Earth Planet. Sci.*, 34, 629–653.
- Hirschmann, M. M., C. Aubaud, and A. C. Withers (2005), Storage capacity of H₂O in nominally anhydrous minerals in the upper mantle, *Earth Planet. Sci. Lett.*, 236(1–2), 167–181.
- Holland, T. J. B., and R. Powell (1998), An internally consistent thermodynamic data set for phases of petrological interest, *J. Metamorph. Geol.*, 16, 309–343.
- Kirby, S. H., W. B. Durham, and L. A. Stern (1991), Mantle phase changes and deep-earthquake faulting in subducting lithosphere, *Science*, 252(5003), 216–225.
- Komabayashi, T., and S. Omori (2006), Internally consistent thermodynamic data set for dense hydrous magnesium silicates up to 35 GPa, 1600°C: Implications for water circulation in the Earth's deep mantle, *Phys. Earth Planet. Inter.*, 156(1–2), 89–107.
- Komabayashi, T., K. Hirose, K.-i. Funakoshi, and N. Takafuji (2005), Stability of phase A in antigorite (serpentine) composition determined by in situ X-ray pressure observations, *Phys. Earth Planet. Inter.*, 151(3–4), 276–289.
- Korenaga, J. (2008), Urey ratio and the structure and evolution of Earth's mantle, *Rev. Geophys.*, 46, RG2007, doi:10.1029/2007RG000241.
- Korenaga, J. (2013), Initiation and evolution of plate tectonics on earth: Theories and observations, *Annu. Rev. Earth Planet. Sci.*, 41(1), 117–151.
- Moresi, L., and M. Gurnis (1996), Constraints on the lateral strength of slabs from three-dimensional dynamic flow models, *Earth Planet. Sci. Lett.*, 138(1–4), 15–28.

- Parai, R., and S. Mukhopadhyay (2012), How large is the subducted water flux? New constraints on mantle regassing rates, *Earth Planet. Sci. Lett.*, *317–318*(0), 396–406.
- Parsons, B., and J. G. Sclater (1977), An analysis of the variation of ocean floor bathymetry and heat flow with age, *J. Geophys. Res.*, *82*(5), 803–827.
- Peacock, S. M., T. Rushmer, and A. B. Thompson (1994), Partial melting of subducting oceanic crust, *Earth Planet. Sci. Lett.*, *121*(1–2), 227–244.
- Ranero, C. R., and V. Sallarès (2004), Geophysical evidence for hydration of the crust and mantle of the Nazca plate during bending at the north Chile trench, *Geology*, *32*(7), 549–552.
- Ranero, C. R., J. Phipps Morgan, K. McIntosh, and C. Reichert (2003), Bending-related faulting and mantle serpentinization at the Middle America trench, *Nature*, *425*(6956), 367–373.
- Ringwood, A. E. (1974), The petrological evolution of island arc systems, *J. Geol. Soc. London*, *130*, 183–204.
- Ritzwoller, M. H., N. M. Shapiro, and S.-J. Zhong (2004), Cooling history of the Pacific lithosphere, *Earth Planet. Sci. Lett.*, *226*(1–2), 69–84.
- Rüpke, L. H., J. P. Morgan, M. Hort, and J. A. D. Connolly (2004), Serpentine and the subduction zone water cycle, *Earth Planet. Sci. Lett.*, *223*(1–2), 17–34.
- Schmidt, M. W., and S. Poli (1998), Experimentally based water budgets for dehydrating slabs and consequences for arc magma generation, *Earth Planet. Sci. Lett.*, *163*(1–4), 361–379.
- Shirey, S. B., B. S. Kamber, M. J. Whitehouse, P. A. Mueller, and A. R. Basu (2008), A review of the isotopic and trace element evidence for mantle and crustal processes in the Hadean and Archean: Implications for the onset of plate tectonic subduction, *Geol. Soc. Am. Spec. Pap.*, *440*, 1–29.
- Smyth, J. R., and S. D. Jacobsen (2006), Nominally anhydrous minerals and Earth's deep water cycle, in *Earth's Deep Water Cycle*, edited by S. D. Jacobsen and S. Van Der Lee, pp. 1–11, AGU, Washington, D. C., doi:10.1029/168GM02.
- Stern, R. J. (2008), Modern-style plate tectonics began in Neoproterozoic time: An alternative interpretation of Earth's tectonic history, *Geol. Soc. Am. Spec. Pap.*, *440*, 265–280.
- Syracuse, E. M., P. E. van Keken, and G. A. Abers (2010), The global range of subduction zone thermal models, *Phys. Earth Planet. Inter.*, *183*(1–2), 73–90.
- Tatsumi, Y., H. Shukuno, K. Tani, N. Takahashi, S. Kodaira, and T. Kogiso (2008), Structure and growth of the Izu-Bonin-Mariana arc crust: 2. Role of crust-mantle transformation and the transparent Moho in arc crust evolution, *J. Geophys. Res.*, *113*, B02203, doi:10.1029/2007JB005121.
- Thompson, A. B. (1992), Water in the Earth's upper mantle, *Nature*, *358*, 295–302.
- van Hunen, J., and A. P. van den Berg (2008), Plate tectonics on the early Earth: Limitations imposed by strength and buoyancy of subducted lithosphere, *Lithos*, *103*(1–2), 217–235.
- van Hunen, J., S. Zhong, N. M. Shapiro, and M. H. Ritzwoller (2005), New evidence for dislocation creep from 3-D geodynamic modeling of the Pacific upper mantle structure, *Earth Planet. Sci. Lett.*, *238*(1–2), 146–155.
- van Keken, P. E. et al. (2008), A community benchmark for subduction zone modeling, *Phys. Earth Planet. Int.*, *171*(1–4), 187–197.
- van Keken, P. E., B. R. Hacker, E. M. Syracuse, and G. A. Abers (2011), Subduction factory: 4. Depth-dependent flux of H₂O from subducting slabs worldwide, *J. Geophys. Res.*, *116*, B01401, doi:10.1029/2010JB007922.
- Wada, I., and K. Wang (2009), Common depth of slab-mantle decoupling: Reconciling diversity and uniformity of subduction zones, *Geochem. Geophys. Geosyst.*, *10*(10), Q10009, doi:10.1029/2009gc002570.
- Wada, I., K. Wang, J. He, and R. D. Hyndman (2008), Weakening of the subduction interface and its effects on surface heat flow, slab dehydration, and mantle wedge serpentinization, *J. Geophys. Res.*, *113*, B04402, doi:10.1029/2007JB005190.
- Wada, I., M. D. Behn, and A. M. Shaw (2012), Effects of heterogeneous hydration in the incoming plate, slab rehydration, and mantle wedge hydration on slab-derived H₂O flux in subduction zones, *Earth Planet. Sci. Lett.*, *353–354*, 60–71.
- Workman, R. K., and S. R. Hart (2005), Major and trace element composition of the depleted MORB mantle (DMM), *Earth Planet. Sci. Lett.*, *231*(1–2), 53–72.
- Zhao, D., Z. Wang, N. Umino, and A. Hasegawa (2009), Mapping the mantle wedge and interplate thrust zone of the northeast Japan arc, *Tectonophysics*, *467*(1–4), 89–106.
- Zhong, S. J., M. T. Zuber, L. Moresi, and M. Gurnis (2000), Role of temperature-dependent viscosity and surface plates in spherical shell models of mantle convection, *J. Geophys. Res.*, *105*(B5), 11,063–11,082.